Volume 1
Number 1
September 2023
Pages 1-124

RSC Applied Polymers

rsc.li/RSCApplPolym

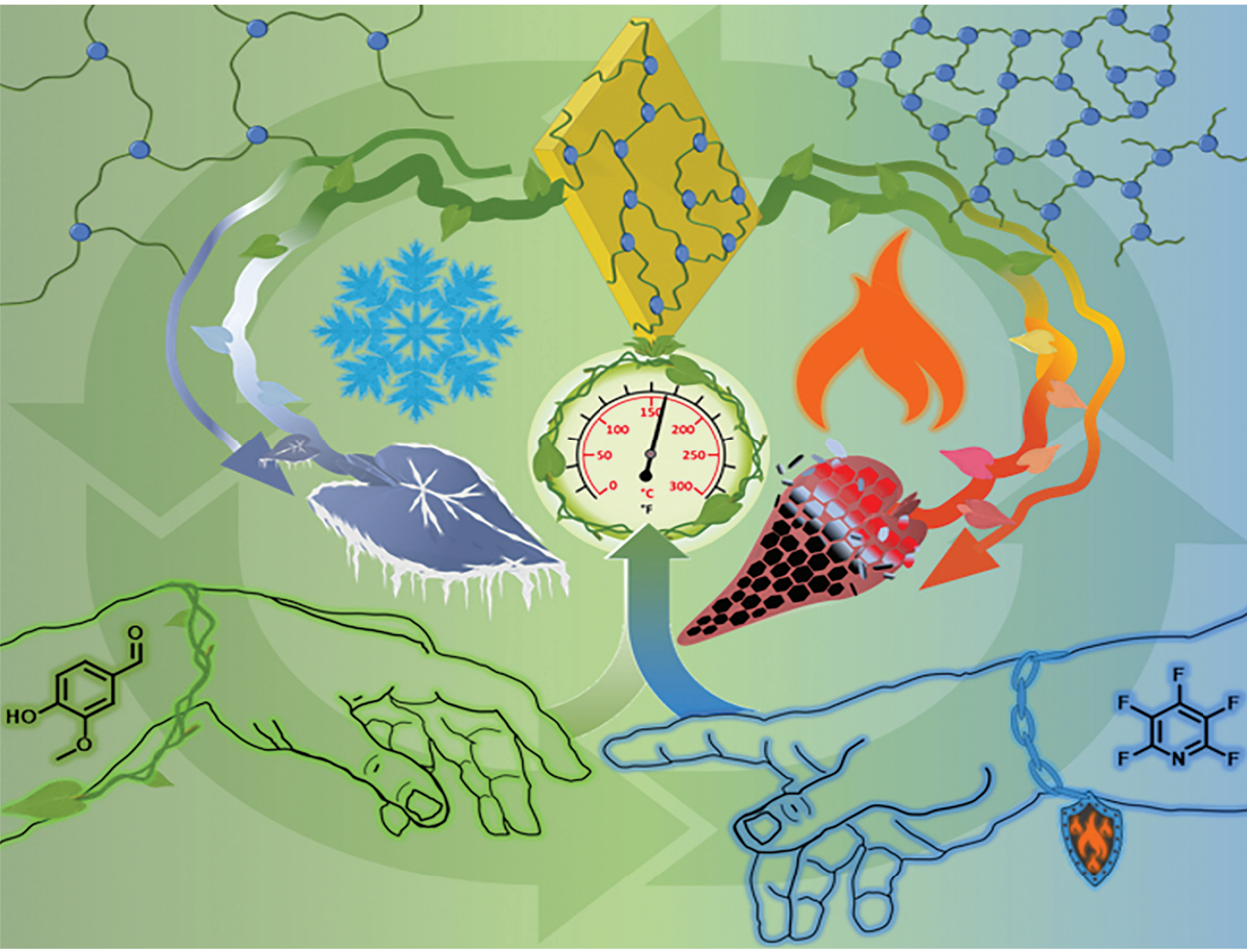

ISSN 2755-371X

ROYAL SOCIETY OF CHEMISTRY

PAPER
Brent S. Sumerlin *et al.*
High-performance polyimine vitrimers from an aromatic bio-based scaffold

RSC Applied Polymers

ROYAL SOCIETY OF CHEMISTRY

PAPER

View Article Online
View Journal | View Issue

Cite this: *RSC Appl. Polym.*, 2023, **1**, 10

High-performance polyimine vitrimers from an aromatic bio-based scaffold†

Kevin A. Stewart, Jacob J. Lessard, Alexander J. Cantor, John F. Rynk, Laura S. Bailey and Brent S. Sumerlin *

Bio-based vitrimers represent a promising class of thermosetting polymer materials, pairing the recyclability of dynamic covalent networks with the renewability of non-fossil fuel feedstocks. Vanillin, a low-cost lignin derivative, enables facile construction of polyimine networks marked by rapid exchange and sensitivity to acid-catalyzed hydrolysis. Furthermore, the aromatic structure makes it a promising candidate for the design of highly aromatic networks capable of high-performance thermal and dimensional stability. Such properties are paramount in polymeric thermal protection systems. Here, we report on the fabrication of polyimine networks with particularly high aromatic content from a novel trifunctional vanillin monomer prepared from the nucleophilic aromatic substitution of perfluoropyridine (PFP) on a multigram scale (>20 g) in high yield (86%). The trifunctional aromatic scaffold was then crosslinked with various diamines to demonstrate tunable viscoelastic behavior and thermal properties, with glass transition temperatures (T_g) ranging from 9 to 147 °C, degradation temperatures (5% mass loss) up to approximately 370 °C, and excellent char yields up to 68% at 650 °C under nitrogen. Moreover, the vitrimers displayed mechanical reprocessability over five destruction/healing cycles and rapid chemical recyclability following acidic hydrolysis at mild temperatures. Our findings indicate that vitrimers possessing tunable properties and high-performance thermomechanical behavior can be easily constructed from vanillin and electrophilic aromatic scaffolds for applications in heat-shielding materials and ablative coatings.

Received 27th April 2023,
Accepted 18th May 2023

DOI: 10.1039/d3lp00019b

rsc.li/rscapplpolym

Introduction

The commercialization of polymers (*i.e.*, plastics) in the century that followed Staudinger's macromolecular hypothesis has brought to fruition rapid societal growth through seemingly endless innovations.[1] Such innovations are seen in nearly every facet of modern-day life, including the aerospace industry.[2] Plastics are lightweight but durable, boasting a wide range of service temperatures and conditions where they remain mechanically and chemically reliable in a host of applications. However, the longevity of many polymeric materials has proven to be a challenge in need of innovation, as the lifetime of many polymers persists well beyond their intended commercial lifecycle,[3] and their manufacturing far exceeds their effective repurposing and remediation.[4] Polymeric materials can be divided into two distinct forms: thermoplastics or thermosets. Thermoplastics are comprised of discrete polymer chains, with interchain connectivity dictated solely by non-covalent interactions and physical entanglements. Given enough energy to disrupt these interactions (typically by heating), the polymer chains can freely flow, allowing thermoplastics to be reshaped and recycled. While these materials are readily recycled and repurposed, the weak interactions between chains often result in fragility under harsh conditions (*e.g.*, heat, chemical, or mechanical stress). This limits many applications, particularly in high-performance uses such as heat-shielding materials (HSMs) or ablatives, which require elevated degradation temperatures and significant formation of inert residual mass following degradation (char yield).[5] Conversely, thermosets are composed of a network of polymer chains are covalently and permanently interconnected. The most predominant polymeric ablatives and HSMs are fabricated using traditional thermosets like silicones, phenolic resins, and ethylene–propylene diene rubber (EPDM), which can be further reinforced with (nano)fillers to augment high-performance behavior.[6–9] As such, assimilating the facile processability and crucial recyclability of thermoplastics with the high-performance capabilities of crosslinked networks remains an important gap to bridge. Liang and coworkers demonstrated that dynamic networks could be efficiently integrated into composite materials that display excellent ablative

George & Josephine Butler Polymer Research Laboratory, Center for Macromolecular Science & Engineering, Department of Chemistry, University of Florida, Gainesville, Florida 32611, USA. E-mail: sumerlin@chem.ufl.edu

†Electronic supplementary information (ESI) available: Synthetic details and complete monomer and vitrimer characterization. See DOI: https://doi.org/10.1039/d3lp00019b

properties.[10] Recently, our group has reported on enaminone-based vitrimer-POSS nanocomposites wherein the POSS filler is the monomeric unit itself, allowing for significantly elevated filler loadings than previously reported. As such, the dynamic ablative networks displayed good shapeability while boasting char yields in excess of 50%.[11]

A combination of the macroscopic reversibility of thermoplastics and the robustness of thermosets now comes in the form of covalent adaptable networks (CANs), a polymer class that has undergone sustained development over the past two decades.[12] The macroscopic flow of CANs is enabled by a dynamic covalent crosslink between the polymer chains. Under specific stimuli (the simplest being heat and/or mechanical force), the crosslink can break and reform allowing macroscopic rearrangement of the polymer chains. Dissociative CANs operate *via* an equilibrium between "open" and "closed" states (*e.g.*, the Diels–Alder adduct).[13] This can result in rapid decreases in viscosity, often (but not invariably[14,15]) due to a concomitant loss in crosslink density as temperature increases.[16–20] On the other hand, associative CANs rely on a new crosslink being formed while another is broken. Associative CANs, often referred to as vitrimers, rely on reactions such as transesterification, transthioetherification, transamination of enaminones, and metathesis of olefins and imines generally showing a linear dependence of viscosity with respect to temperature.[21–29] This linear dependence is a result of the degenerative exchange mechanism, leading to consistency in crosslink density at any temperature and predictable viscoelastic behavior based on bond exchange or architecture of building blocks.[30,31]

Recent interest has focused on the amplification of the promising sustainability of vitrimers by utilizing bio-based building blocks to fabricate these dynamic networks.[32–40] The ability to synthesize a useful polymer from a renewable resource is an obvious benefit. As such, bio-based CANs are an attractive platform for designing sustainable, high-performance materials.[41–44] Some of the most popular and well-explored natural feedstock chemicals for designing CANs are furfural derivatives, epoxidized vegetable and castor oil derivatives, cellulose, Priamine mixtures, and vanillin – a phenolic monomer sourced from lignin.[45–48] Vanillin is cost-effective and offers both a nucleophilic handle to fabricate multifunctional monomers and an activated aldehyde to synthesize polyimine vitrimers under straightforward, catalyst-free conditions. A further advantage to bio-derived vitrimers is the exchange chemistries that enable viscous flow often being susceptible to mild chemical degradation.[35,49,50] In this way, an enhanced decay of the materials may ultimately allow for efficient breakdown into its bio-sourced monomeric units. In particular, the imine bond is hydrolytically labile under mildly acidic conditions, offering a viable end-of-life treatment process for disposal.

The aromaticity of vanillin is well-matched for designing network materials capable of elevated thermal resistance and greater dimensional stability that can offset some of the inherent drawbacks of dynamically crosslinked polymers (*i.e.*, material creep or deformation over time).[51–53] Additionally, the nucleophilic phenol can be leveraged to construct monomers of highly aromatic nature from the nucleophilic aromatic substitution (S_NAR) of scaffolds such as trichlorotriazine (TCT) and perfluoropyridine (PFP), which have been demonstrated as valuable building blocks for polymer functionalization and high-performance materials.[54–59]

In this report, we demonstrate that polyimine vitrimers with high-performance thermal stability and charring behavior can be conveniently fabricated from fully aromatic trifunctional monomers from the S_NAR of PFP and vanillin. We further demonstrate that both the viscoelastic and thermal behavior of the vitrimers can be easily modified by changing the identity of the diamine used to crosslink the trifunctional vanillin platform. These high bio-mass (>90 wt%) networks feature excellent thermal stabilities, outstanding charring behavior, and effective mechanical reprocessability and chemical recyclability – making them promising candidates for biomass-derived HSMs.

Results and discussion

Synthesis and characterization of bio-derived monomer and vitrimers

To fabricate polyimine vitrimers possessing robust thermal and dimensional stability, PFP was utilized as a scaffold for synthesizing a highly aromatic, semi-fluorinated trialdehyde monomer. PFP was reacted with 3.2 equiv of vanillin, comparable to literature conditions reported for similar PFP-based systems (Fig. 1).[6,60] The reaction was conveniently monitored by ^{19}F NMR spectroscopy, showing rapid progression to the disubstituted product within 3 h, followed by a slower conversion to the trisubstituted ring after 8 h, a result of fluorine displacement and subsequent deactivation of the ring electrophilicity (Fig. S1†). The product (TVnFP) was prepared on a multi-gram scale with high yields and excellent purity after recrystallization (Fig. S2–S5†). The synthesis can also be achieved using the more inexpensive potassium carbonate, albeit in lower yields (62%). Gratifyingly, the high biomass percentage (80 wt%) TVnFP is readily solubilized in common organic solvents such as dichloromethane (DCM), chloroform, and tetrahydrofuran, allowing for simple preparation of polyimine networks with particularly high aromatic character.

Subsequently, the vitrimers were synthesized *via* catalyst-free condensation between TVnFP and four commercially available diamines: *m*-xylylenediamine (X), hexamethylenediamine (H), diaminododecane (D), and Priamine 1074 (P), chosen to demonstrate tunable thermal and viscoelastic properties (Fig. S6A and S7†). To favor a predominantly imine metathesis exchange mechanism over transamination, we maintained a 1 : 1 molar ratio of amine to aldehyde across all network formulations. In this way, the rapid dynamics of the network operating under transamination pathways can be slowed such that susceptibility to creep can be abated.[42] The vitrimers were prepared by solution casting from DCM, to provide optimal

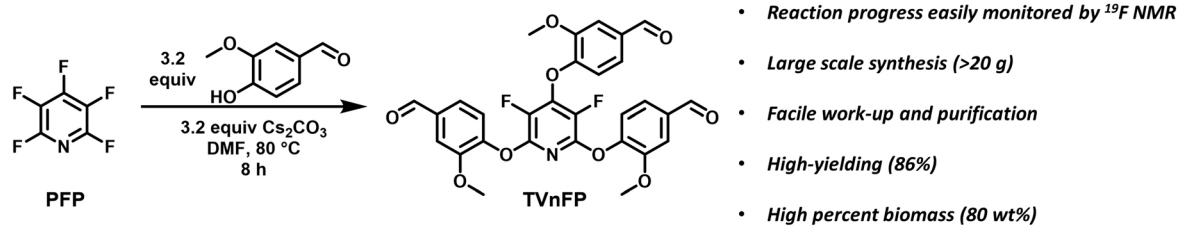

Fig. 1 Synthetic scheme and conditions with key features of tris(vanillyl)-3,5-difluoropyridine (TVnFP) monomer synthesis.

phase compatibility and mechanical properties.[61] Specifically in the condensation between TVnFP and X, the DCM-swollen organogel was not dried completely prior to curing to foam under reduced pressure (Fig. S6A–E†). We anticipated the TVn-X network would possess a potentially prohibitively high T_g for the efficient healing large fragments, thus a powderized network with a significantly increased surface area would provide optimal healing of the processed material.[62] Conversely, the condensations of TVnFP with H, D, and P were allowed to evaporate fully before curing, resulting in free-standing, flexible vitrimer films (Fig. S8A–C and S9†). The vitrimers were compression molded into disk and bar geometries at elevated temperatures and under reduced pressure. After 2 h, completely healed materials with excellent transparency and minimal defects were obtained (Fig. 2A–D).

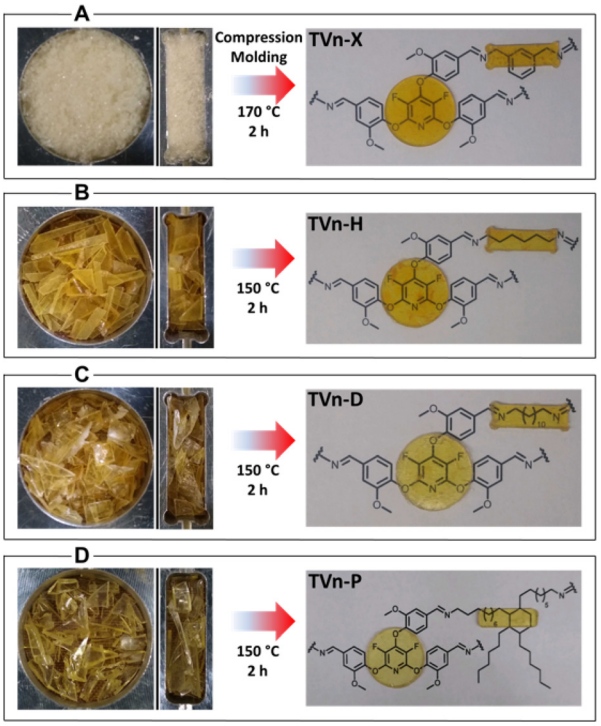

Fig. 2 Compression molding of vitrimer particles from networks of trivanillin monomer crosslinked with (A) *m*-xylylenediamine (TVn-X), (B) hexamethylenediamine (TVn-H), (C) diaminododecane (TVn-D), and (D) Priamine (TVn-P). Resultant disk and bar geometries indicate excellent healability with minimal defects and high transparency.

The vitrimers were then characterized by differential scanning calorimetry (DSC), thermogravimetric analysis (TGA), FT-IR spectroscopy, dynamic mechanical analysis (DMA), and shear rheology. DSC analysis showed T_g values ranging from 147 to 9 °C, decreasing with higher aliphatic content (Fig. 3A and Fig. S15–S18†). As expected, the TVn-X vitrimer had a notably high T_g value at nearly 150 °C, supporting the anticipated benefit of small particle size during processing. FTIR spectroscopy of all vitrimers showed complete disappearance of the C=O stretching of the aldehyde at ~1690 cm^{-1} and the appearance of the C=N stretching of the imine at ~1648 cm^{-1} (Fig. 3B; Fig. S10–S14†). Subsequent TGA analysis of the vitrimers showed excellent thermal stability, with onset decomposition temperatures (temperature at 5% mass loss, $T_{d,5\%}$) ranging from 301 to 366 °C (Fig. 4). Interestingly, TVn-P possessed the highest decomposition temperature, even when compared to TVn-X, which we expected to be the most robust vitrimer system. However, the TVn-P system undergoes an abrupt decomposition to its residual char, whereas the TVn-X and -H systems exhibit a uniquely gradual decomposition profile up to a temperature of 650 °C. Moreover, the TVn-H vitrimer displayed a noticeably lower $T_{d,5\%}$ and $T_{d,10\%}$ compared to the other systems, perhaps due to incomplete network formation. After comparing the virgin TVn-H to the same vitrimer after five reprocess cycles, the onset degradation temperature increased to 322 °C (Fig. S19†). Gratifyingly, the TVn-X and -H display outstanding char yields at 650 °C of 68 and 55%, respectively. Predictably, the char yields decreased substantially as the aliphatic character increased, with residual masses of 36 and 15% for TVn-D and -P, respectively. To the best of our knowledge, TVn-X exhibits the highest char yield of any reported vanillin-based polyimine vitrimer to date, suggesting that these vitrimer systems are excellent candidates for ablative materials. Selected properties of the vitrimers are summarized in Table S1.†

Rheological and mechanical characterization

The vitrimers were subsequently characterized by DMA and shear rheology. All three formulations displayed rubbery plateaus (constant storage moduli past T_g) in the DMA thermograms, characteristic of constant crosslink density over the entire test. T_g values, measured at the peak of tan(δ), agreed with those evidenced by DSC (Fig. 5A–D and Fig. S20–S31†). Yet, owing to the exceedingly high T_g of TVn-X, the rubbery plateau of the vitrimer was notably short within the selected

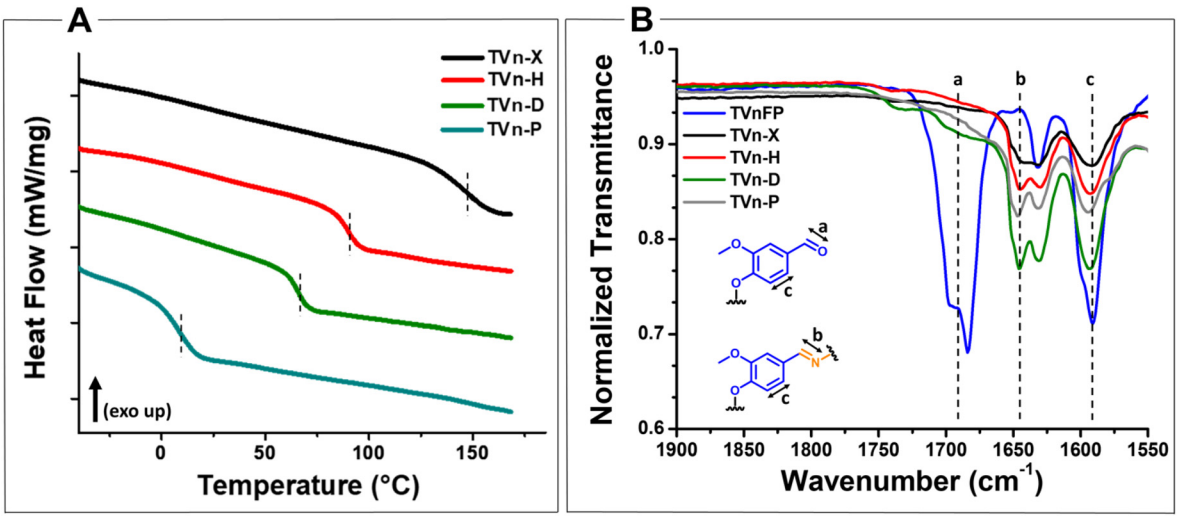

Fig. 3 (A) Stacked differential scanning calorimetry (DSC) plots with marked T_g values of networks crosslinked with *m*-xylylenediamine (TVn-X), hexamethylenediamine (TVn-H), diaminododecane (TVn-D), and Priamine (TVn-P) showing excellent tunability over a wide temperature range. (B) Overlayed FTIR spectra of vitrimers with trivanillin monomer (TVnFP), indicating near full disappearance of the aldehyde carbonyl stretch and clear emergence of characteristic imine stretch.

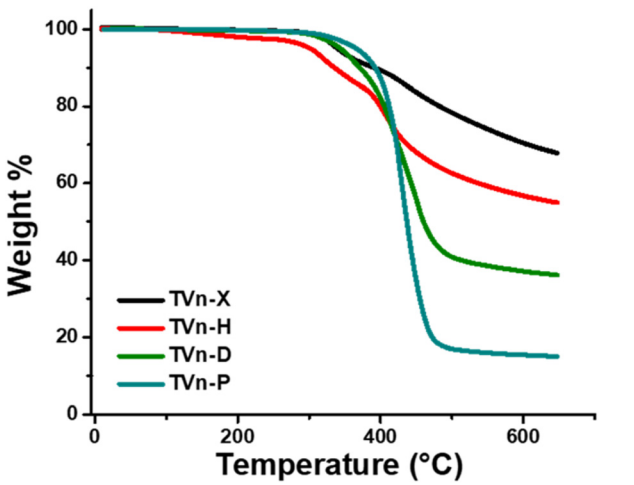

Fig. 4 Thermogravimetric analysis (TGA) plots (under N_2) of networks crosslinked with *m*-xylylenediamine (TVn-X), hexamethylenediamine (TVn-H), diaminododecane (TVn-D), and Priamine (TVn-P) indicating excellent stability and outstanding charring behavior.

temperature range of the measurement, warranting a subsequent temperature sweep above 200 °C.

Remarkably, when the temperature range was increased to 260 °C, the TVn-X vitrimer displayed a dramatic increase in the storage modulus (Fig. S34A†). This high-temperature phenomenon was further verified by DSC analysis, which exhibited a clear exothermic event occurring at approximately 200–250 °C after only one heating cycle (Fig. S34B†). Interestingly, the increase in storage modulus at elevated temperatures was minor for TVn-H, and the DSC thermogram displayed a similar exotherm at slightly higher temperatures; however, this event was present during all three heating cycles and led to a patent, consistent increase in the apparent T_g (Fig. S35A and B†). Furthermore, TVn-D and -P displayed no notable increase in storage modulus at elevated temperatures and presented no apparent exothermic event at the same temperatures (Fig. S36A, B and S37A, B†). We hypothesize that as the network density/free volume increases with respect to length and flexibility of the diamine crosslinker, the proximity of any free amine and the unreacted C–F bonds of the fluoropyridine ring increases. Thus, at temperatures exceeding approximately 185–200 °C (roughly the onset of the exothermic events of XDA and HMDA, respectively), any residual unreacted amines undergo S_NAR with the C–F sites on the fluoropyridine ring resulting in permanent crosslinks that increase the crosslink density and T_g of the networks. However, the lengthy spacers of TVn-D and -P effectively eliminate this bulk phenomenon. Regardless, the secondary reaction occurring in the TVn-X vitrimer acts as a self-reinforcement mechanism at elevated temperatures to further enhance the thermal robustness of the network, as indicated by its strikingly slow degradation profile.

Creep-recovery experiments were conducted at 150 °C under a constant force of 5000 Pa for 400 s followed by a recovery time of 200 s to probe network susceptibility to deformation at an elevated temperature. All vitrimer formulations evidenced significant permanent deformation (Fig. 6A). Unsurprisingly, the vitrimers' propensity to deformation increased as the T_g of the material decreased. TVn-X and TVn-H exhibited similar recovery, but when the diamine was dramatically increased in length with TVn-D and -P, the recovery was diminished altogether (Table S2†). While the deformation drastically increased for TVn-P at this temperature, it is worth noting that the permanent deformation was consistent at lower temperatures (Fig. S33†). Thus, processing of TVn-P can be easily achieved with lower energy expenditure. In short, the vitrimers

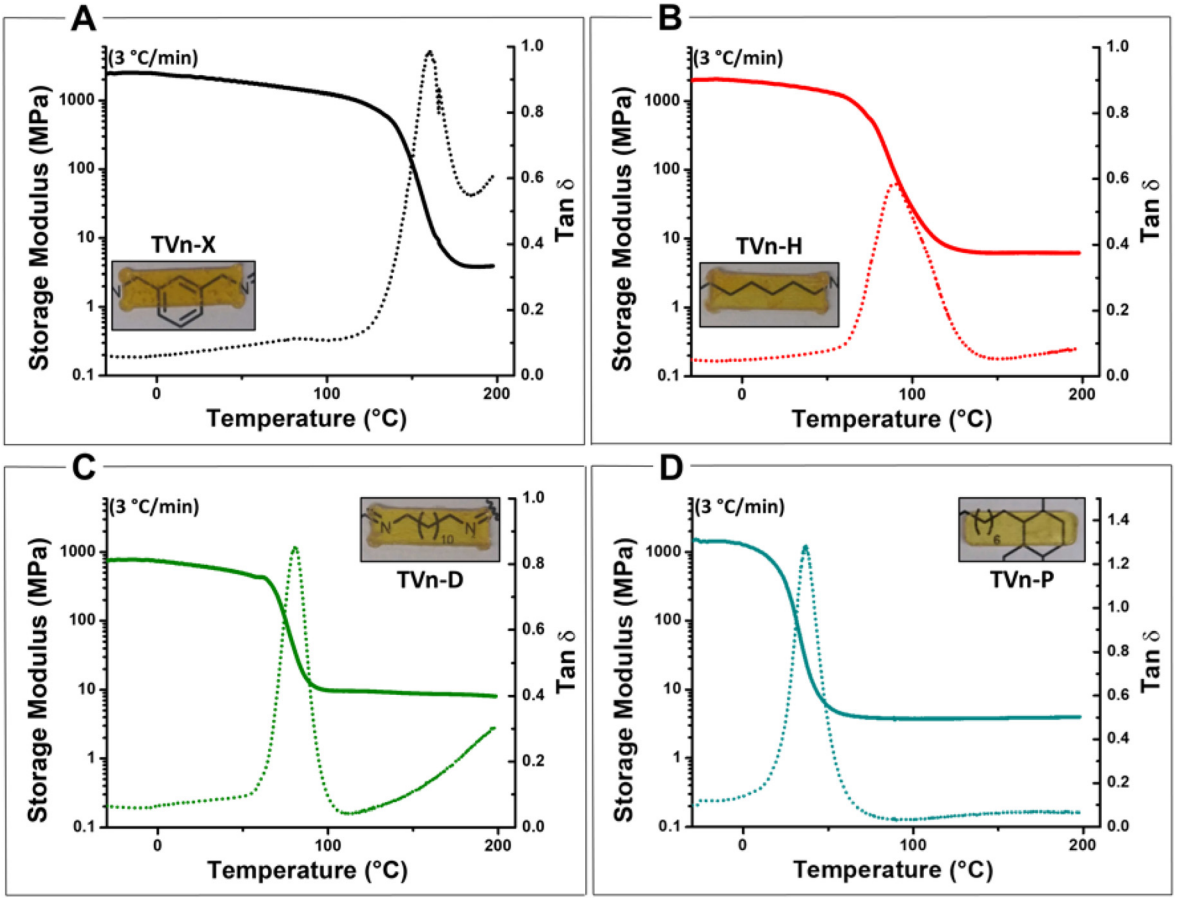

Fig. 5 DMA thermograms of networks crosslinked with (A) *m*-xylylenediamine (TVn-X), (B) hexamethylenediamine (TVn-H), (C) diaminododecane (TVn-D), and (D) Priamine (TVn-P) showing tan(δ) peaks consistent with T_g values from DSC and constant rubbery plateau moduli indicating constant crosslink density. Inset images of vitrimer bar used in experiments.

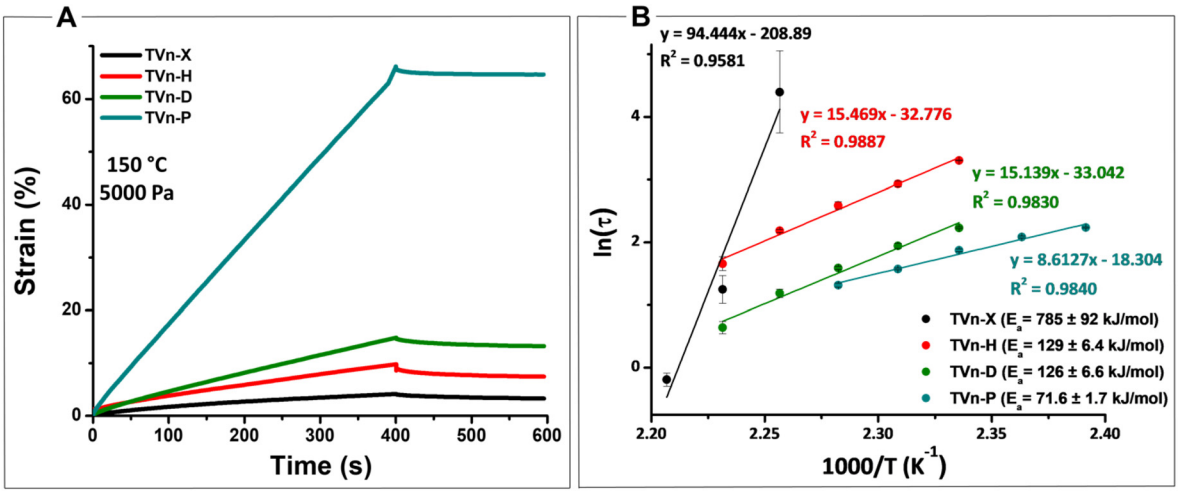

Fig. 6 (A) Creep-recovery experiments for networks crosslinked with *m*-xylylenediamine (TVn-X), hexamethylenediamine (TVn-H), diaminododecane (TVn-D), and Priamine (TVn-P) at 150 °C at a constant force of 5000 Pa (experiments ran in duplicate). (B) Arrhenius plots of stress relaxation data for networks (τ at G/G_0 = 1/*e*, in 5 °C increments). Data indicates flow behavior is dependent on diamine functionality. Vitrimer samples in triplicate.

displayed predictable creep behavior, with TVn-X displaying outstanding resistance to deformation at elevated temperatures.

Stress relaxation experiments displayed similar trends between vitrimer formulations as those evidenced by creep-recovery experiments. The temperature sensitivity of the networks, or the energy of activation for viscous flow (E_a), scaled similarly with the length and flexibility of the diamine. E_a values of 785, 129, 126, and 71.6 kJ mol^{-1} for TVn-X, -H, -D, and -P, respectively, were generated after fitting the data to Arrhenius' law (Fig. 6B and eqn (S1)†). The extraordinarily high E_a value for TVn-X was likely a result of the competitive reaction occurring simultaneously, leading to appreciable levels of irreversible crosslinking at high temperatures. Thus, at 170 °C the characteristic relaxation time dramatically increased, and at 165 °C the vitrimer was incapable of reaching 1/e of the initial relaxation modulus leading to the markedly high (and likely inaccurate) E_a of TVn-X (Fig. S32A†). Finally, it is worth noting that the E_a values of TVn-H and -D are quite similar, indicating that the networks are similarly sensitive to temperature, owing to the similarity of the diamines. However, the characteristic relaxation times of TVn-H are patently higher than those of TVn-D at all temperatures, a result of the differences in T_g between these two materials (Fig. S32B and C†). This was further supported by the lower E_a and relaxation times of TVn-P (Fig. S32D†). These results indicate the viscoelastic behavior (creep resistance and temperature sensitivity) can be predictably altered, allowing for vitrimer networks with tailorable flow behavior and thermomechanical strength.

Finally, we investigated the tensile behavior of the TVn-P vitrimer, as it displayed promising elastomeric properties. Tensile specimens were compression molded at 150 °C for 2 h under reduced pressure, and the samples were tested until failure (in triplicate). The vitrimer displayed good extensibility and moderate tensile strength at room temperature, with average stress and strain at break of 2.9 ± 0.78 MPa and 87 ± 18%, respectively (Fig. S38 and S39†). Thus, the TVnFP monomer shows promising utility for fabricating renewable, polyimine elastomers with excellent thermal stability. We anticipated the extensibility of the TVn-X, -H, and -D vitrimers would decrease significantly as a result of their T_g values, so these materials were not considered for further tensile characterization.

Reprocessability and chemical degradability

In regard to sustainability, the capacity of vitrimers to be damaged, healed, and repetitively reprocessed is arguably their most defining characteristic – made particularly appealing when the material is heavily biomass-derived. As such, the reprocessability of the TVnFP networks was examined by performing DMA experiments over multiple destruction/healing cycles. The initial TVn-X vitrimer bar (tested up to 200 °C) was capable of being sufficiently healed, with some surface defects, while maintaining good transparency (Fig. S43A†). However, a rubbery plateau was not evidenced within the temperature sweep range, and the T_g increased dramatically – further supporting the presence of the proposed secondary reaction resulting in permanent crosslink formation (Fig. S40A†). The remaining formulations possessed efficient recyclability over five reprocess cycles with minor defects accumulated and a consistent darkening in color, likely due to oxidation of imines or residual amines (Fig. S43B–D†). Additionally, they displayed consistent increases in T_g and rubbery plateau moduli after each healing cycle, with TVn-H and TVn-P showing the largest deviations from the virgin material over the reprocessing sequence (Fig. S40B–D†). Finally, FTIR spectroscopy of the reprocessed vitrimers indicated good retention of characteristic stretches as the virgin material (Fig. S44–S47†). With the exception of XDA, the vitrimers displayed respectable recyclability over several destruction and healing steps.

Dynamic covalent crosslinks enable efficient end-of-life remediation owing to the susceptibility of the exchangeable bond to chemical reversibility, further bolstering the sustainable nature of CANs as promising commodity plastics. Networks comprised of imine crosslinks enable rapid and efficient hydrolytic degradation under mildly acidic conditions and can be further accelerated by elevated temperatures. Thus, the virgin TVnFP vitrimers were immersed in 0.1 M HCl at room temperature for 48 h (Fig. S48A, B and S49B, C†). TVn-H and -P displayed noticeable degradation under these conditions, whereas TVn-X and -D appeared mostly unaffected. However, upon heating to 60 °C, all four networks appeared to fully degrade, and an off-white precipitate was observed (Fig. S48C and S49D†). Gratifyingly, ^{1}H NMR and ^{19}F NMR analysis showed that the harvested precipitates were indeed TVnFP (Fig. S50 and S51†). Thus, the TVnFP vitrimers were demonstrated to undergo efficient and repetitive mechanical recyclability, generally maintaining the properties of the parent material (with the exception of TVn-X), and all four vitrimers were capable of rapid chemical degradability under mildly acidic conditions.

Conclusion

The preparation of value-added polymer materials from renewable resources is a promising avenue for combating the escalating obstacle of sustainability in plastic manufacturing. However, the ability to design bio-based polymers with notable high-performance properties worthy of ablative applications remains an important challenge. The materials in this report offer a facile route to high aromatic-content polyimine vitrimers that demonstrate rapid processability, adjustable T_g over a range of nearly 150 °C, excellent thermal stabilities up to nearly 370 °C, and outstanding charring behavior attributed to a secondary crosslinking event that occurs during thermal degradation. The networks indicated tunable creep-recovery profiles and Arrhenius-dependent flow behavior. Finally, the networks displayed both mechanical reprocessability and chemical recyclability under mildly acidic conditions. Our

findings are an encouraging addition to the growing field of bio-based vitrimers, demonstrating that vanillin can be readily incorporated with high-performance constituent elements such as PFP to design shapeable, recyclable, and easily remediated thermoset materials with augmented thermomechanical characteristics.

Conflicts of interest

There are no conflicts to declare.

Acknowledgements

This material is based upon work supported by the National Science Foundation (NSF DMR-1904631). MS was performed by the UF Mass Spectrometry Research and Education Center, supported by funding from the National Institute of Health (S10 OD021758-01A1 and S10 OD030250-01A1). We thank Anton Paar for the use of the Anton Paar 702 rheometer through their VIP academic program.

Notes and references

1 H. Staudinger, Über Polymerisation, *Ber. Dtsch. Chem. Ges. A/B*, 1920, **53**, 1073–1085, DOI: **10.1002/cber.19200530627**.
2 M. Natali, J. M. Kenny and L. Torre, Science and Technology of Polymeric Ablative Materials for Thermal Protection Systems and Propulsion Devices: A Review, *Prog. Mater. Sci.*, 2016, **84**, 192–275, DOI: **10.1016/j.pmatsci.2016.08.003**.
3 R. C. Hale, A. E. King, J. M. Ramirez, M. La Guardia and C. Nidel, Durable Plastic Goods: A Source of Microplastics and Chemical Additives in the Built and Natural Environments, *Environ. Sci. Technol. Lett.*, 2022, **9**, 798–807, DOI: **10.1021/acs.estlett.2c00417**.
4 J. M. Millican and S. Agarwal, Plastic Pollution: A Material Problem?, *Macromolecules*, 2021, **54**, 4455–4469, DOI: **10.1021/acs.macromol.0c02814**.
5 K. George, B. P. Panda, S. Mohanty and S. K. Nayak, Recent Developments in Elastomeric Heat Shielding Materials for Solid Rocket Motor Casing Application for Future Perspective, *Polym. Adv. Technol.*, 2018, **29**, 8–21, DOI: **10.1002/pat.4101**.
6 K. A. Stewart, D. Shuster, M. Leising, I. Coolidge, E. Lee, C. Stevens, A. J. Peloquin, D. Kure, A. R. Jennings and S. T. Iacono, Synthesis, Characterization, and Thermal Properties of Fluoropyridyl-Functionalized Siloxanes of Diverse Polymeric Architectures, *Macromolecules*, 2021, **54**, 4871–4879, DOI: **10.1021/acs.macromol.1c00333**.
7 M. Natali, M. Monti, D. Puglia, J. M. Kenny and L. Torre, Ablative Properties of Carbon Black and MWNT/Phenolic Composites: A Comparative Study, *Composites, Part A*, 2012, **43**, 174–182, DOI: **10.1016/j.compositesa.2011.10.006**.
8 S. Eismeier, A. J. Peloquin, K. A. Stewart, C. A. Corley and S. T. Iacono, Pyridine-Functionalized Linear and Network Step-Growth Fluoropolymers, *J. Fluor. Chem.*, 2020, **238**, 109631, DOI: **10.1016/j.jfluchem.2020.109631**.
9 J. Li, B. Hu, K. Hui, K. Li and L. Wang, Effects of Inorganic Nanofibers and High Char Yield Fillers on Char Layer Structure and Ablation Resistance of Ethylene Propylene Diene Monomer Composites, *Composites, Part A*, 2021, **150**, 106633, DOI: **10.1016/j.compositesa.2021.106633**.
10 Y. Cai, H. Zou, S. Zhou, Y. Chen and M. Liang, Room-Temperature Self-Healing Ablative Composites via Dynamic Covalent Bonds for High-Performance Applications, *ACS Appl. Polym. Mater.*, 2020, **2**, 3977–3987, DOI: **10.1021/acsapm.0c00638**.
11 K. A. Stewart, D. P. Delellis, J. J. Lessard, J. F. Rynk and B. S. Sumerlin, Dynamic Ablative Networks: Shapeable Heat-Shielding Materials, *ACS Appl. Mater. Interfaces*, 2023, **15**, 25212–25223, DOI: **10.1021/acsami.2c22924**.
12 G. M. Scheutz, J. J. Lessard, M. B. Sims and B. S. Sumerlin, Adaptable Crosslinks in Polymeric Materials: Resolving the Intersection of Thermoplastics and Thermosets, *J. Am. Chem. Soc.*, 2019, **141**, 16181–16196, DOI: **10.1021/jacs.9b07922**.
13 X. Chen, M. A. Dam, K. Ono, A. Mal, H. Shen, S. R. Nutt, K. Sheran and F. Wudl, A Thermally Re-Mendable Cross-Linked Polymeric Material, *Science*, 2002, **295**, 1698–1702, DOI: **10.1126/science.1065879**.
14 S. Mondal, J. J. Lessard, C. L. Meena, G. J. Sanjayan and B. S. Sumerlin, Janus Cross-Links in Supramolecular Networks, *J. Am. Chem. Soc.*, 2022, **144**, 845–853, DOI: **10.1021/jacs.1c10606**.
15 L. Zhang and S. J. Rowan, Effect of Sterics and Degree of Cross-Linking on the Mechanical Properties of Dynamic Poly(Alkylurea-urethane) Networks, *ACS Macro Lett.*, 2017, **50**, 5051–5060, DOI: **10.1021/acs.macromol.7b01016**.
16 M. Liu, J. Zhong, Z. Li, J. Rong, K. Yang, J. Zhou, L. Shen, F. Gao, X. Huang and H. He, A High Stiffness and Self-Healable Polyurethane Based on Disulfide Bonds and Hydrogen Bonding, *Eur. Polym. J.*, 2020, **124**, 109475, DOI: **10.1016/j.eurpolymj.2020.109475**.
17 B. R. Elling and W. R. Dichtel, Reprocessable Cross-Linked Polymer Networks: Are Associative Exchange Mechanisms Desirable?, *ACS Cent. Sci.*, 2020, **6**, 1488–1496, DOI: **10.1021/acscentsci.0c00567**.
18 J. M. Winne, L. Leibler and F. E. Du Prez, Dynamic Covalent Chemistry in Polymer Networks: A Mechanistic Perspective, *Polym. Chem.*, 2019, **10**, 6091–6108, DOI: **10.1039/c9py01260e**.
19 E. E. L. Maassen, J. P. A. Heuts and R. P. Sijbesma, Reversible Crosslinking and Fast Stress Relaxation in Dynamic Polymer Networks via Transalkylation Using 1,4-Diazabicyclo[2.2.2] Octane, *Polym. Chem.*, 2021, **12**, 3640–3649, DOI: **10.1039/d1py00292a**.
20 S. Wang, Y. Yang, H. Ying, X. Jing, B. Wang, Y. Zhang and J. Cheng, Recyclable, Self-Healable, and Highly Malleable Poly(Urethane-Urea)s with Improved Thermal and

Mechanical Performances, *ACS Appl. Mater. Interfaces*, 2020, **12**, 35403–35414, DOI: 10.1021/acsami.0c07553.

21 J. L. Self, C. S. Sample, A. E. Levi, K. Li, R. Xie, J. R. De Alaniz and C. M. Bates, Dynamic Bottlebrush Polymer Networks: Self-Healing in Super-Soft Materials, *J. Am. Chem. Soc.*, 2020, **142**, 7567–7573, DOI: 10.1021/jacs.0c01467.

22 J. S. A. Ishibashi and J. A. Kalow, Vitrimeric Silicone Elastomers Enabled by Dynamic Meldrum's Acid-Derived Cross-Links, *ACS Macro Lett.*, 2018, **7**, 482–486, DOI: 10.1021/acsmacrolett.8b00166.

23 J. J. Lessard, L. F. Garcia, C. P. Easterling, M. B. Sims, K. C. Bentz, S. Arencibia, D. A. Savin and B. S. Sumerlin, Catalyst-Free Vitrimers from Vinyl Polymers, *Macromolecules*, 2019, **52**, 2105–2111, DOI: 10.1021/acs.macromol.8b02477.

24 J. J. Lessard, G. M. Scheutz, R. W. Hughes and B. S. Sumerlin, Polystyrene-Based Vitrimers: Inexpensive and Recyclable Thermosets, *ACS Appl. Polym. Mater.*, 2020, **2**, 3044–3048, DOI: 10.1021/acsapm.0c00523.

25 Y. Lu and Z. Guan, Olefin Metathesis for Effective Polymer Healing via Dynamic Exchange of Strong Carbon–Carbon Double Bonds, *J. Am. Chem. Soc.*, 2012, **134**, 14226–14231, DOI: 10.1021/ja306287s.

26 P. Taynton, K. Yu, R. K. Shoemaker, Y. Jin, H. J. Qi and W. Zhang, Heat- or Water-Driven Malleability in a Highly Recyclable Covalent Network Polymer, *Adv. Mater.*, 2014, **26**(23), 3938–3942, DOI: 10.1002/adma.201400317.

27 S. K. Schoustra, T. Groeneveld and M. M. J. Smulders, The Effect of Polarity on the Molecular Exchange Dynamics in Imine-Based Covalent Adaptable Networks, *Polym. Chem.*, 2021, **12**, 1635–1642, DOI: 10.1039/d0py01555e.

28 S. Wang, L. Li, Q. Liu and M. W. Urban, Self-Healable Acrylic-Based Covalently Adaptable Networks, *Macromolecules*, 2022, **55**, 4703–4709, DOI: 10.1021/acs.macromol.2c00739.

29 S. Wang, L. Li and M. W. Urban, Combined Reprocessability and Self-Healing in Fluorinated Acrylic-Based Covalent Adaptable Networks (CANs), *ACS Appl. Polym. Mater.*, 2022, **4**, 9360–9367, DOI: 10.1021/acsapm.2c01609.

30 J. J. Lessard, G. M. Scheutz, S. H. Sung, K. A. Lantz, T. H. Epps and B. S. Sumerlin, Block Copolymer Vitrimers, *J. Am. Chem. Soc.*, 2020, **142**, 283–289, DOI: 10.1021/jacs.9b10360.

31 J. J. Lessard, K. A. Stewart and B. S. Sumerlin, Controlling Dynamics of Associative Networks through Primary Chain Length, *Macromolecules*, 2022, **55**, 10052–10061, DOI: 10.1021/acs.macromol.2c01909.

32 M. A. Lucherelli, A. Duval and L. Avérous, Biobased Vitrimers: Towards Sustainable and Adaptable Performing Polymer Materials, *Prog. Polym. Sci.*, 2022, **127**, 101515, DOI: 10.1016/j.progpolymsci.2022.101515.

33 L. Imbernon, E. K. Oikonomou, S. Norvez and L. Leibler, Chemically Crosslinked yet Reprocessable Epoxidized Natural Rubber via Thermo-Activated Disulfide Rearrangements, *Polym. Chem.*, 2015, **6**, 4271–4278, DOI: 10.1039/c5py00459d.

34 T. Liu, C. Hao, L. Wang, Y. Li, W. Liu, J. Xin and J. Zhang, Eugenol-Derived Biobased Epoxy: Shape Memory, Repairing, and Recyclability, *Macromolecules*, 2017, **50**, 8588–8597, DOI: 10.1021/acs.macromol.7b01889.

35 H. Geng, Y. Wang, Q. Yu, S. Gu, Y. Zhou, W. Xu, X. Zhang and D. Ye, Vanillin-Based Polyschiff Vitrimers: Reprocessability and Chemical Recyclability, *ACS Sustainable Chem. Eng.*, 2018, **6**, 15463–15470, DOI: 10.1021/acssuschemeng.8b03925.

36 W. Zhao, Z. Feng, Z. Liang, Y. Lv, F. Xiang, C. Xiong, C. Duan, L. Dai and Y. Ni, Vitrimer-Cellulose Paper Composites: A New Class of Strong, Smart, Green, and Sustainable Materials, *ACS Appl. Mater. Interfaces*, 2019, **11**, 36090–36099, DOI: 10.1021/acsami.9b11991.

37 X. Yang, L. Guo, X. Xu, S. Shang and H. Liu, A Fully Bio-Based Epoxy Vitrimer: Self-Healing, Triple-Shape Memory and Reprocessing Triggered by Dynamic Covalent Bond Exchange, *Mater. Des.*, 2020, **186**, 1–10, DOI: 10.1016/j.matdes.2019.108248.

38 J. Wu, X. Yu, H. Zhang, J. Guo, J. Hu and M.-H. Li, Fully Biobased Vitrimers from Glycyrrhizic Acid and Soybean Oil for Self-Healing, Shape Memory, Weldable, and Recyclable Materials, *ACS Sustainable Chem. Eng.*, 2020, **8**, 6479–6487, DOI: 10.1021/acssuschemeng.0c01047.

39 S. Debnath, S. Kaushal and U. Ojha, Catalyst-Free Partially Bio-Based Polyester Vitrimers, *ACS Appl. Polym. Mater.*, 2020, **2**, 1006–1013, DOI: 10.1021/acsapm.0c00016.

40 Y. Zhu, F. Gao, J. Zhong, L. Shen and Y. Lin, Renewable Castor Oil and DL-Limonene Derived Fully Bio-Based Vinylogous Urethane Vitrimers, *Eur. Polym. J.*, 2020, **135**, 109865, DOI: 10.1016/j.eurpolymj.2020.109865.

41 S. Wang, S. Ma, Q. Li, X. Xu, B. Wang, W. Yuan, S. Zhou, S. You and J. Zhu, Facile In Situ Preparation of High-Performance Epoxy Vitrimer from Renewable Resources and Its Application in Nondestructive Recyclable Carbon Fiber Composite, *Green Chem.*, 2019, **21**, 1484–1497, DOI: 10.1039/c8gc03477j.

42 H. Memon, H. Liu, M. A. Rashid, L. Chen, Q. Jiang, L. Zhang, Y. Wei, W. Liu and Y. Qiu, Vanillin-Based Epoxy Vitrimer with High Performance and Closed-Loop Recyclability, *Macromolecules*, 2020, **53**, 621–630, DOI: 10.1021/acs.macromol.9b02006.

43 Y. Tao, L. Fang, M. Dai, C. Wang, J. Sun and Q. Fang, Sustainable Alternative to Bisphenol A Epoxy Resin: High-Performance Recyclable Epoxy Vitrimers Derived from Protocatechuic Acid, *Polym. Chem.*, 2020, **11**, 4500–4506, DOI: 10.1039/d0py00545b.

44 Z. Su, S. Huang, Y. Wang, H. Ling, X. Yang, Y. Jin, X. Wang and W. Zhang, Robust, High-Barrier, and Fully Recyclable Cellulose-Based Plastic Replacement Enabled by a Dynamic Imine Polymer, *J. Mater. Chem. A*, 2020, **8**, 14082–14090, DOI: 10.1039/d0ta02138e.

45 S. Dhers, G. Vantomme and L. Avérous, A Fully Bio-Based Polyimine Vitrimer Derived from Fructose, *Green Chem.*, 2019, **21**, 1596–1601, DOI: 10.1039/c9gc00540d.

46 A. Zych, J. Tellers, L. Bertolacci, L. Ceseracciu, L. Marini, G. Mancini and A. Athanassiou, Biobased, Biodegradable, Self-Healing Boronic Ester Vitrimers from Epoxidized Soybean Oil Acrylate, *ACS Appl. Polym. Mater.*, 2020, **3**, 1135–1144, DOI: **10.1021/acsapm.0c01335**.

47 J. L. Swartz, R. L. Li and W. R. Dichtel, Incorporating Functionalized Cellulose to Increase the Toughness of Covalent Adaptable Networks, *ACS Appl. Mater. Interfaces*, 2020, **12**, 44110–44116, DOI: **10.1021/acsami.0c09215**.

48 C. Taplan, M. Guerre and F. E. Du Prez, Covalent, Adaptable Networks Using β-Amino Esters as Thermally Reversible Building Blocks, *J. Am. Chem. Soc.*, 2021, **143**, 9140–9150, DOI: **10.1021/jacs.1c03316**.

49 Z. Zhou, X. Su, J. Liu and R. Liu, Synthesis of Vanillin-Based Polyimine Vitrimers with Excellent Reprocessability, Fast Chemical Degradability, and Adhesion, *ACS Appl. Polym. Mater.*, 2020, **2**, 5716–5725, DOI: **10.1021/acsapm.0c01008**.

50 Y. Tao, L. Fang, J. Zhou, C. Wang, J. Sun and Q. Fang, Gel–Sol Transition of Vanillin-Based Polyimine Vitrimers: Imparting Vitrimers with Extra Welding and Self-Healing Abilities, *ACS Appl. Polym. Mater.*, 2020, **2**, 295–303, DOI: **10.1021/acsapm.9b00809**.

51 M. D. Garrison, M. A. Savolainen, A. P. Chafin, J. E. Baca, A. M. Bons and B. G. Harvey, Synthesis and Characterization of High-Performance, Bio-Based Epoxy-Amine Networks Derived from Resveratrol, *ACS Sustainable Chem. Eng.*, 2020, **8**, 14137–14149, DOI: **10.1021/acssuschemeng.0c04816**.

52 K. Hong, Q. Sun, X. Zhang, L. Fan, T. Wu, J. Du and Y. Zhu, Fully Bio-Based High-Performance Thermosets with Closed-Loop Recyclability, *ACS Sustainable Chem. Eng.*, 2022, **10**, 1036–1046, DOI: **10.1021/acssuschemeng.1c07523**.

53 M. G. Mohamed, C. J. Li, M. A. R. Khan, C. C. Liaw, K. Zhang and S. W. Kuo, Formaldehyde-Free Synthesis of Fully Bio-Based Multifunctional Bisbenzoxazine Resins from Natural Renewable Starting Materials, *Macromolecules*, 2022, **55**, 3106–3115, DOI: **10.1021/acs.macromol.2c00417**.

54 C. A. Figg, T. Kubo and B. S. Sumerlin, Efficient and Chemoselective Synthesis of ω,ω-Heterodifunctional Polymers, *ACS Macro Lett.*, 2015, **4**, 1114–1118, DOI: **10.1021/acsmacrolett.5b00634**.

55 T. Kubo, C. A. Figg, J. L. Swartz, W. L. A. Brooks and B. S. Sumerlin, Multifunctional Homopolymers: Postpolymerization Modification via Sequential Nucleophilic Aromatic Substitution, *Macromolecules*, 2016, **49**, 2077–2084, DOI: **10.1021/acs.macromol.6b00181**.

56 T. Kubo, K. C. Bentz, K. C. Powell, C. A. Figg, J. L. Swartz, M. Tansky, A. Chauhan, D. A. Savin and B. S. Sumerlin, Modular and Rapid Access to Amphiphilic Homopolymers: Via Successive Chemoselective Post-Polymerization Modification, *Polym. Chem.*, 2017, **8**, 6028–6032, DOI: **10.1039/c7py01585b**.

57 M. B. Houck, L. C. Brown, R. H. Lambeth and S. T. Iacono, Exploiting the Site Selectivity of Perfluoropyridine for Facile Access to Densified Polyarylene Networks for Carbon-Rich Materials, *ACS Macro Lett.*, 2020, **9**, 964–968, DOI: **10.1021/acsmacrolett.0c00298**.

58 M. B. Houck, T. J. Fuhrer, C. R. Phelps, L. C. Brown and S. T. Iacono, Toward Taming the Chemical Reversibility of Perfluoropyridine through Molecular Design with Applications to Pre-and Postmodifiable Polymer Architectures, *Macromolecules*, 2021, **54**, 5586–5594, DOI: **10.1021/acs.macromol.1c00990**.

59 C. M. Friesen, A. R. Kelley and S. T. Iacono, Shaken Not Stirred: Perfluoropyridine-Polyalkylether Prepolymers, *Macromolecules*, 2022, **55**, 10970–10979, DOI: **10.1021/acs.macromol.2c01310**.

60 L. M. J. Moore, K. T. Greeson, K. A. Stewart, D. A. Kure, C. A. Corley, A. R. Jennings, S. T. Iacono and K. B. Ghiassi, Perfluoropyridine as a Scaffold for Semifluorinated Thiol-Ene Networks with Readily Tunable Thermal Properties, *Macromol. Chem. Phys.*, 2020, **221**, 1–5, DOI: **10.1002/macp.202000100**.

61 C. Zhu, C. Xi, W. Doro, T. Wang, X. Zhang, Y. Jin and W. Zhang, Tuning the Physical Properties of Malleable and Recyclable Polyimine Thermosets: The Effect of Solvent and Monomer Concentration, *RSC Adv.*, 2017, **7**, 48303–48307, DOI: **10.1039/c7ra10956c**.

62 L. Yu, C. Zhu, X. H. Sun, J. Salter, H. A. Wu, Y. Jin, W. Zhang and R. Long, Rapid Fabrication of Malleable Fiber Reinforced Composites with Vitrimer Powder, *ACS Appl. Polym. Mater.*, 2019, **1**, 2535–2542, DOI: **10.1021/acsapm.9b00641**.